OXFORD JOURNAL
OF STUDENT
SCHOLARSHIP

Linear Quadratic Regulator based Controller Design for Vertical Attitude Adjustment with Thrust Vectoring

Seif Shebl
seif.shebl@icloud.com

ABSTRACT

This study investigates the control and adjustment of an aerospace airfoil's vertical attitude in a flow field through Linear Quadratic Regulator controller design and Thrust Vector Control methods. Types of thrust vector control and controllers are investigated and evaluated against each other through the study of the thrust and aerodynamic drag forces acting on the airfoil. The system is modelled through derivations of an airfoil's equations of motion used to calculate values for the state-space representation of the dynamic system. Thereby, allowing for a state-feedback loop to form through the LQR framework, computing gain values to re-stabilise the rigid body system. Once the controller is demonstrated and illustrates a high level of optimal outputs which are efficient, the controller's robustness is tested through altering initial system parameters and the state variables physical values. Reliably, the LQR controller provided a consistent energy efficient output.

Keywords

Vertical orientation; Rocket attitude control; Rocket efficiency; Trajectory; Thrust vector control; State-space modelling; Torque; Structural stability; Structural failure; Linear quadratic regulator (LQR); Rocket stabilisation; Altitude control systems; Centre of mass; Gimbaling engines; Movable fins; Vernier rockets; Canards; Vanes; Attitude-control rockets; Gimbaled engine; Hydraulic and electric actuators; Gimbal angle; Proportional integral derivative (PID)

INTRODUCTION

The Significance of Rockets to Maintain their Vertical Orientation Precisely During Launch

It is crucial for rockets to maintain their vertical orientation during launch, as this will optimise the rocket's efficiency and allow it to remain stable during the early ascent phase. As the rocket climbs in altitude, there are a number of external forces that can be taken to act on its fuselage. The four forces include but are not limited to thrust, weight, lift and drag. As these forces act on the rocket's fuselage, they can cause it to deviate off of its precisely calculated flight plan (Jang et al., 2011). Therefore, altering

its trajectory or completely subverting its orientation in the flow field (Aerotecnica Missili & Spazio, 2023).

Implementing control systems will allow the rocket to actively govern its orientation. This is to ensure that the vertical position is maintained for the greatest duration possible. Furthermore, if the rocket remains vertical during launch, the horizontal component of the thrust force acting on its body will be minimised (Sopegno et al., 2023). Thus, ensuring that there is no torque moment perpendicular to its direction of travel and the efficiency is maximised. If these forces were to act perpendicular to the centre of mass, it could cause bending stresses on the materials. Thereby, degrading its structural stability, and in extreme cases, causing complete structural failure as the breaking stress of the materials are exceeded (NASA, 2021). Additionally, as the vertical component of the upwards force is maximised, it allows the resultant force incident on the fuselage to remain parallel to the rocket's structural axis. This ensures that there are no moments about the centre of mass.

It is important to note that building an efficient rocket is only part of the problem: maintaining safety is equally as important. Attitude control systems will allow the rocket to fly steadily in an unvarying direction. Whereas, the omittance of such systems will cause it to follow unpredictable trajectories. This can pose legitimate flight risks to people on board and on the ground (NASA, 2021).

Vertical Orientation

The vertical orientation of an airfoil refers to its longitudinal axis in a flow field being perpendicular to the ground during launch. This means thrust acts directly downwards opposing the gravitational force only and no additional aerodynamic forces (ERAU, 2022 - 2026). Ensuring this orientation is maintained during its launch is crucial for efficiency and structural stability. By guaranteeing the thrust acts directly under the airfoil's central axes, we ensure that the work done against gravity is maximised, reducing the volume of wasted fuel. Additionally, the direction thrust acts in governs the aerodynamic forces acting on the fuselage (Jang et al., 2011). When the thrust is perfectly aligned with the airfoil's longitudinal axis no aerodynamic forces act on its body, so no loads are placed on the outer materials which could cause catastrophic failure (Ekanayake, 2026; Patel et al., 2025).

The Significance of the Study

The study will significantly contribute both to the aerospace industry and to the analysis of control systems, addressing the particular problem of maintaining an airfoil's vertical orientation in a flow field precisely. Rockets are innately unstable launch vehicles which can follow unpredictable trajectories due to even the most minor deviation in attitude. Therefore, the implementation of attitude controllers is critical to ensure trajectory deviations are diminished, minimal forces act as a component on the rocket's fuselage and the vehicle is efficiently optimised throughout its entire journey.

From a control systems approach, the administration of accurate attitude controllers, such as Proportional-Integral-Derivative (PID) and Linear Quadratic Regulator (LQR) Controllers, provide a

systematic and robust technique to regulate dynamic systems quickly and efficiently (Patel et al., 2026). This efficiency is especially important in the industry as unnecessary movements produced by attitude control attempts from Thrust Vector Control (TVC) will lead to increased fuel consumption and costs. In addition, while current research either focuses on highly intricate and detailed control systems or TVC there is a shortfall in the integration of control system frameworks in modern dynamic airfoil systems. This study narrows this gap by developing a simplified yet diligent model for optimal controller design in these modern systems (Patel et al., 2025).

Aims and Goals of the Paper

The specific aim of this paper is to create an LQR model to analyse and control the motion of an airfoil during flight. This involves deriving equations of motion, and implementing state space representation to simultaneously model how the variables influence each other in one cohesive system.

The study seeks to investigate how the variables: pitch, pitch rate, cart position and cart velocity affect each other over time in a dynamic system. This was especially in response to forces which create a disturbance torque moment about the center of gravity. The state space representation will enable us to calculate the required moment and angular acceleration (Patel et al., 2026). In doing so, the gimbal angle to regain vertical orientation is found. Furthermore, the implementation of the LQR in code allows the research to demonstrate how closed feedback loops can be used. By using current values for the state variables the loop can continuously provide a new output until equilibrium is reached, highlighting how the LQR provides an efficient and robust control method which optimises its output to require minimal effort and its ability to stabilise dynamic multi-variable systems.

LITERATURE REVIEW

Aerodynamics and Drag

The aerodynamic forces acting on the rocket during launch are dominated by various forms of drag, which can influence the vehicle's performance drastically. During the initial launch phase, where the rocket has the smallest vertical height, air density is greatest. Therefore, parasitic drag is substantial. Parasitic drag can be categorised into types and includes skin friction drag, form drag and interference drag caused by resistance (friction) with the air field brought primarily by the materials used and the fuselage's shape. The drag equation states - $D = (\frac{1}{2})\rho v^2 C_d A$, where ρ is the density of surrounding air, v is the velocity of the object relative to the fluid, A is the reference area, and C_d is the drag coefficient (GU Rocketry, 2021). Therefore, it can be deduced that as the density is decreased the drag force acting decreases. Hence parasitic drag is greatest near the ground. Moreover, one of the main design goals in modern rocketry is to minimise the drag coefficient of aerial vehicles (Patel & Ansell, 2023). The drag coefficient associates a numerical dimensionless value with how streamlined an object is, as this coefficient decreases the object is said to be more streamlined, accordingly aerospace engineers try to

design rockets with the goal of reducing the drag coefficient and therefore aerodynamic resistive forces (SimScale, n.d.).

This can be achieved through aerodynamic optimisation, such as implementing the correct airfoil geometry, reducing surface texture and roughness, and meticulously designing external rocket components to limit the separation of flow and skin friction drag (Patel & Ansell, 2023). The shape of the fuselage has a massive impact on its drag coefficient (SimScale, n.d.). Different geometries interact distinctively with fluids, where streamlined shapes such as teardrops or airfoils are designed to minimise drag by guiding the fluid around itself. Blunt objects, such as boxes often create two opposing areas of pressure (high and low) leading to flow separation. (NASA, 2025)

Thrust

It is crucial to understand how the rocket produces thrust, as this influences the type of TVC which can be utilised. A rocket produces thrust through the combustion of fuel where it is pressurised with oxygen in the combustion chamber producing pressurised gas due to the narrowing of its diameter. This gas accelerates out from the exhaust nozzle. Thus, creating a resultant force that is greater than the weight of the rocket. Due to Newton's 2nd law of motion, $F = m \times a$, the rocket accelerates (NASA, 2021). Solid propellant rocket engines have no restart capability. Once burning begins, the fuel will combust until completely used up, as there is no way to stop propellant flow. Whereas, liquid propellant engines provide enhanced throttle control and restart capability, as the fuel flow rate can be managed or even completely stopped (Sutton & Biblarz, 2017). Therefore, solid propellant engines require more demanding controls from the TVC system, reducing coherence and cost-effectiveness **(**ERAU, 2022 - 2026**)**.

The thrust equation is as follows: $T = \dot{m}v_e + (p_e - p_a)A_e$, where $\dot{m}$ is the mass flow rate, p_e is the exhaust pressure, p_a is the atmospheric pressure, v_e is velocity, and A is the nozzle exit area. The mass flow rate is the mass of fluid (fuel) passing a cross sectional area per unit time (NASA, 2021). If the mass of fluid passing through an area per unit time is increased, mass flow rate will increase and therefore thrust increases. Governing control over the magnitude and direction of thrust will allow you to create the most reliable and efficient control system (Patel et al., 2025). Therefore, liquid propellant engines are far more superior to create launch vehicles which have more meticulous and precise control systems.

History of Rockets

The development of rockets dates back to the year 1232, where the first rocket was reportedly used. However, it was not for its modern intended sense of space exploration. The Chinese were testing the use of tubes enclosed at one end and filled with gun powder. By combusting the powder, highly pressurised gas was accelerated out the open end of the tube propelling the contraption forwards. It was highly unstable and had no means of stability control. In saying that, it was the first true solid propellant engine to be produced.

The first ever attempt to launch a liquid-propellant rocket was in 1926 when Robert H. Goddard designed, constructed and launched his very own rocket in Auburn, Massachusetts. It featured a nozzle and combustion chamber which when enough fuel was combusted allowed the rocket to successfully launch. Goddard's main goal was to prove that liquid-propellant based rockets offered the greatest potential and would be the benchmark for the future of space travel. Modern research supports Goddard's claim, as liquid-propellant engines give us far better control of the attitude of the launch vehicle in a flow field (NASA, 2021).

Components of a Rocket

Modern rockets consist of 4 different systems - the propulsion system, payload system, guidance system and the structural system. Understanding how they are designed is crucial, as they control the rocket's attitude, structural integrity and ability to withstand shear forces acting on its body. The structural integrity of a body refers to its ability to withstand loading forces without breaking or deformation. In the case of an aerial vehicle these forces include the components of thrust and drag that act perpendicular to the fuselage's surface. The structural system refers to the frame of the rocket, which is comparable to the fuselage of an airplane. It is made from materials with impeccable strength to weight ratios, such as aluminum or titanium. These outer panels (skin) are joined together by using inner hoops which have stringers going lengthwise down the entire rocket, throughout the whole circumference of the hoops (NASA, 2023). The nose cone is the very top of the rocket. Therefore, it is the first component affected by airflow. Consequently, the shape of the nose cone has a massive contribution to the aerodynamic efficiency of the rocket (Apogee Components, n.d.).

There are many shapes which are mathematically optimal, each shape designed depending on the rocket's payload weight and speed requirements (Apogee Components, n.d.). The Ogive shape resembling a rounded teardrop is the most common for rockets which travel through subsonic and transonic speeds (0.5-1.2 mach) as it offers balance between minimised drag and mass manufacturability. Whereas, the Von Kármán shape resembling a smooth pointed tip is optimised for supersonic speeds (1.5-5 mach) providing the lowest possible drag. In saying that, it may be deemed more difficult to manufacture (Richard Nakka, 2023).

The guidance system is responsible for ensuring the rocket maintains the correct flight path to reach its destination. Through precise computer numerical calculations the system is able to identify the exact position, velocity, pitch and acceleration of the vehicle using sensors, such as inertial measurement units (IMU's), gyroscopes, accelerometers and barometric altimeters (Jang et al, 2011). Through using data collated from these sensors, they compared the required variables with their current states. By using a closed feedback loop, they calculated the required input to achieve the required trajectory. Then, these inputs are delegated to the TVC systems integrated in the rocket (Sutton & Biblarz, 2017). The input calculated from the closed feedback loop can be sent to actuators or motors connected to these control methods.

The Main Technologies

Control systems, such as Thrust Vector Control (TVC), has been widely implemented into many modern rockets as a method to direct the attitude of the thrust force produced from the engines. Thereby, creating a restorative torque moment about the centre of mass (CM). This can combat the disturbance moment, returning the fuselage to the desired vertical orientation by regulating its rotation in the yaw and pitch axes (Aerotecnica Missili & Spazio, 2023). TVC does not refer to one mechanism, rather it is a group of different control techniques which can be chosen based on the required needs. The main types of TVC are: gimbaling engines, movable fins, vernier rockets, canards, vanes and attitude-control rockets (Sheth et al, 2024; CalAcademy, n.d.).

With a gimbaled engine, the exhaust nozzle is able to swivel in all directions. Thus, redirecting the flow of exhaust gases and the thrust force produced by the engine. As the thrust force is at an angle to the centre of mass it creates a torque moment, which is able to restabilise the rocket's orientation (NASA, 2021). The nozzle is made to swivel using hydraulic or electric actuators which use calculation produced from a feedback controller to regulate the extent of the gimbal angle.

Feedback controllers, such as Proportional integral derivative (PID) or Linear quadratic regulator (LQR), are used for this feedback loop. This is where they take the rockets' initial states and input them into a dynamic mathematical model to provide a set of outputs. This will allow the vertical orientation to be achieved with minimal effort. PID controllers are feedback loop mechanisms that analyse current variable data and command TVC systems to make adjustments allowing the variable to reach a setpoint (Åström, 2002). The LQR controller is also a feedback loop mechanism. However, it depends on a mathematical model to predict and produce the most optimized output (ScienceDirect, n.d.).

Some rockets employ movable fins which are positioned at the bottom of the rocket's fuselage. These fins move through electric motors, and are able to redistribute the flow of aerodynamic forces, lift and drag from the surrounding airflow. The point at which these aerodynamic forces act is called the centre of pressure (CP), and for a restorative moment to be produced the CP must be below the CM (NASA, 2023). The CP can be ensured to be below the CM as the fins are positioned near the bottom of the fuselage, increasing the drag. Thus, shifting it downwards. Other methods, such as vernier rockets, implement smaller thrusters on the base of the fuselage near the main engines. These thrusters produce a torque moment which restabilises the rocket on its pitch and yaw axis (NASA, 2023; Sopegno, L et al. (2023).

METHODOLOGY

In this study, the subject under consideration is the case of an airfoil in a flow field that is treated as a rigid body which can experience minor angular deflections from its centre of mass. Thus, forming a dynamic counterpart of the well-known inverted pendulum problem (Patel et al., 2026). In addition, the airfoil experiences a thrust force along its longitudinal axis in atmospheric pressure under the influence of gravity. It is assumed that the rocket is placed on a base that confines its motion in the vertical direction

only. Whilst, rotation around the CM is free. A constant exhaust flow causes the thrust action, and it is comparable to freestream velocity in standard aerodynamic airfoil systems. This is where any minor perturbation in orientation will create a restorative or nonrestorative moment. This is depending on whether the thrust acts perpendicular or parallel to the rocket's axis of symmetry. In addition, the base is virtual. Therefore, the base has no effect on propulsion flow (Patel et al., 2025).

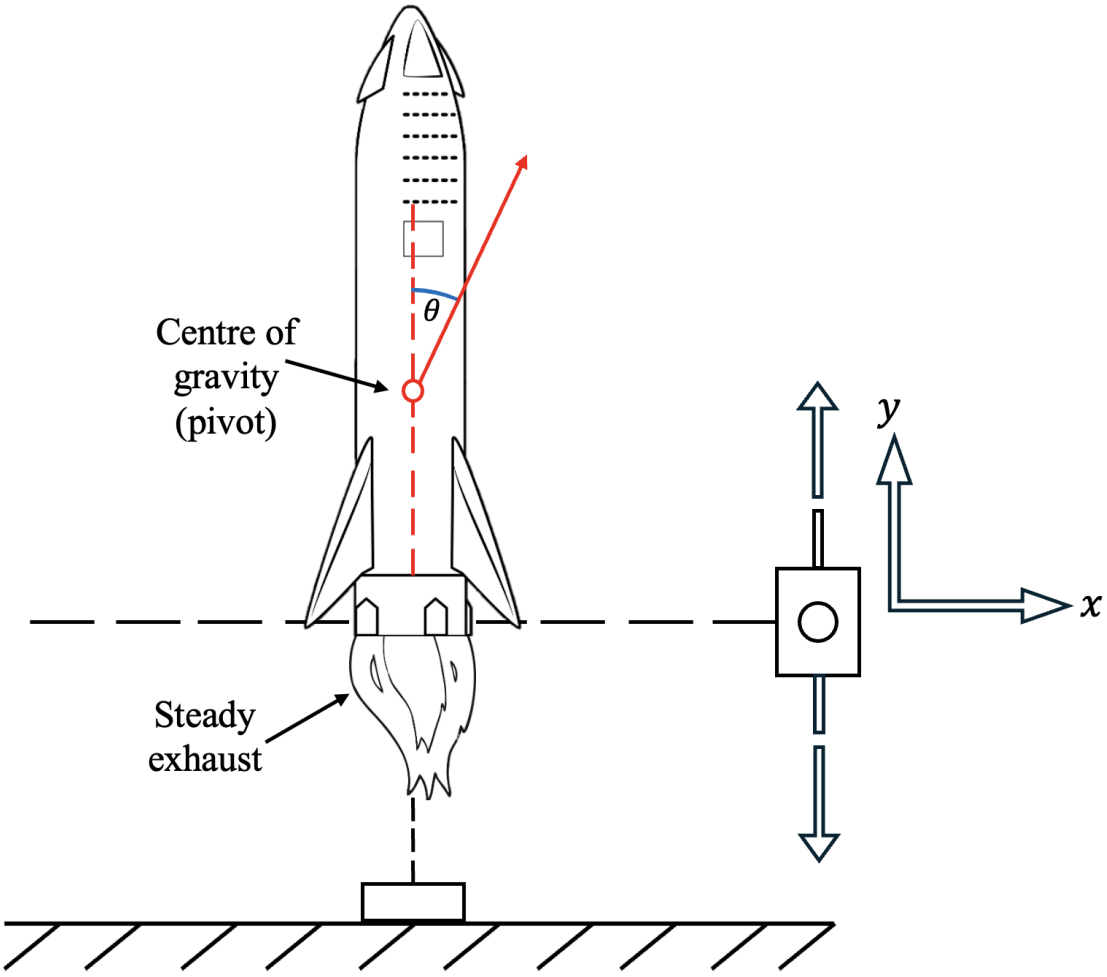

Figure 1: Schematic of the vertically launched rocket system. Motion of the rocket is limited to the vertical y-direction by the virtual base, while free to sway horizontally at the base due to small angular deviations about the CM.

Due to forces acting perpendicular to the rocket's fuselage (parallel to the ground), small deviations in the orientation of the vehicle occur. Therefore, causing pitch deviations from the central vertical. Sensors detect the shift in attitude and calibrate the TVC systems to regain the vertical position. The force and speed at which the TVC executes these demands depends primarily on the pitch rate and moment of inertia. This means how quickly the angular deviation is occurring and how easy its rotation may be

altered. Furthermore, this change in pitch impacts the cart position (Patel et al., 2026). Therefore, the system is classified as having two degrees-of-freedom.

The moment of inertia (I_G) is a physical quantity measuring the defiance of an object to change its rotational speed. The greater the I_G of an object the harder it is to stop and start rotating in addition to changing its rotational speed.

Deriving The Equations of Motion

The model considers a dynamic and rigid body framework where the movement of the system is determined by the angle of pitch and vertical movement. The equations of motion are established based on Newton's laws of motion. Some simplifying assumptions are made to ensure that the system can remain tractable to be analysed for control purposes (Patel et al., 2026). The resulting equations of motion are expressed in state space form. The system can be modelled as an airfoil which can rotate from its trailing edge. In addition, a uniform gravitational field is assumed, so the centre of mass and centre of gravity coincide and are at the same position.

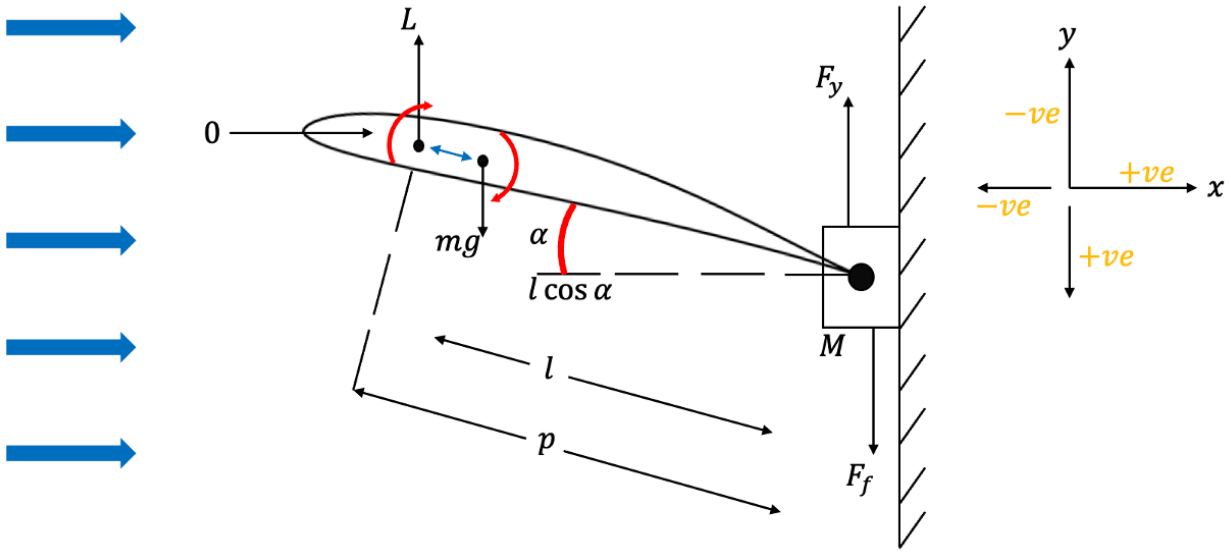

Figure 2: showcasing the schematic of an airfoil in a flow field. Where l is the distance from the CM to the pivot M, a is the pitch (angular deviation) of the airfoil, p is the distance from the aerodynamic centre to the pivot, L is the lift force and F_y is the vertical component of force

Considering the free body diagram of the airfoil:

The horizontal position of the airfoils centre of mass relative to the pivot point, based on the length of the airfoil l and pitch angle α is:

$$x_G = -l \cos \alpha$$

The vertical position of the airfoil's centre of mass is defined as the sum of the original displacement of the base and vertical component of displacement due to the rotary motion is:

$$y_G = y + l \sin \alpha$$

Taking the second derivatives of these equations allows us to obtain the acceleration, which is required for Newton's second law ($F = Ma$). The airfoil experiences a heaving and rotational motion in the dynamic system. Therefore, these double derivatives reveal important physical effects, such as angular acceleration (pitch rate) and rotational (centripetal) acceleration. This is where l is the distance from the pivot to the CM, and α is the angle of attack of the airfoil with freestream velocity:

$$\frac{d^2 x_G}{dt^2} = l[\sin \alpha \frac{d^2 \alpha}{dt^2} + \cos \alpha \left(\frac{d\alpha}{dt}\right)^2]$$
$$\frac{d^2 y_G}{dt^2} = \frac{d^2 y}{dt^2} + l[\cos \alpha \frac{d^2 \alpha}{dt^2} - \sin \alpha \left(\frac{d\alpha}{dt}\right)^2]$$

Next, we take the sum of the forces in the x and y direction as Newton's 2nd law states the net resultant force acting on a body is its $mass \times acceleration$. There are multiple forces acting on the airfoil, so by summing these forces we are able to account for the coupling effect they have on each other:

$$F_y = -L + mg + m\frac{d^2 y}{dt^2} + ml\cos \alpha \frac{d^2 \alpha}{dt^2} - ml\sin \alpha \left(\frac{d\alpha}{dt}\right)^2$$
$$F_x = 0 - ml\sin \alpha \frac{d^2 \alpha}{dt^2} - ml\cos \alpha \left(\frac{d\alpha}{dt}\right)^2$$

Where F_y is the sum of all forces acting vertically (Y-direction), L is the lift force, mg is the weight of the mass, $m\frac{d^2 y}{dt^2}$ is the vertical acceleration of the cart, $ml\cos \alpha \frac{d^2 \alpha}{dt^2}$ is the vertical component of angular acceleration, $ml\sin \alpha \left(\frac{d\alpha}{dt}\right)^2$ is the centripetal acceleration term, F_x is the sum of all forces acting horizontally (X-direction), $ml\sin \alpha \frac{d^2 \alpha}{dt^2}$ is the horizontal force due to angular acceleration and $ml\cos \alpha \left(\frac{d\alpha}{dt}\right)^2$ is the centripetal force component.

For the vertical motion of the airfoil, Newton's second law can be written as:

$$M\frac{d^2 y}{dt^2} = F_v - F_y - b\frac{dy}{dt} - Mg$$

Where F_v is a constant vertical force to account for gust or wind disturbances, and b is the frictional coefficient, which acts as a damping term opposing the motion of the cart. The greater the displacement and acceleration, the larger the frictional coefficient acting upon the system.

Substituting the value of F_y into this equation provides:

$$(M + m)\frac{d^2y}{dt^2} = L + F_v - b\frac{dy}{dt} - (M + m)g - ml[\frac{d^2\alpha}{dt^2}cos\,\alpha - (\frac{d\alpha}{dt})^2 sin\,\alpha]$$

Where $(M + m)$ is the total total mass of the system and $\frac{d^2y}{dt^2}$ is the acceleration in the Y-direction. When these variables are multiplied, according to Newton's second law force in the Y-direction is found, L is the external lift force, F_v is the damping force which is proportional to the velocity ($\frac{dy}{dt}$) and the entire term $ml[\frac{d^2\alpha}{dt^2}cos\,\alpha - (\frac{d\alpha}{dt})^2 sin\,\alpha]$ represents how the centripetal rotation of the rigid body affects the cart's vertical motion. This equation portrays how the vertical displacement of the cart is affected by external forces, and how the total combined mass of the cart and airfoil system accelerates under these forces, damping coefficients and coupling effects of rotation.

The relationship between the moment applied on an airfoil and its angular acceleration is represented by:

$$\sum \tau = I\ddot{\alpha} = I\frac{d^2\alpha}{dt^2}$$

Where $\sum \tau$ is the sum of moments acting about the pivot, $\ddot{\alpha}$ is the angular acceleration of the airfoil in the flow field, and I is the moment of inertia. A few assumptions are made for tractability. Drag is neglected for simplicity. Therefore, the moments considered are only due to forces F_x , F_y and lift (Patel et al., 2026).

Therefore, the sum of moments can be taken to be the lift moment, horizontal force contribution and vertical force contribution. This equation relates the torque applied on the system with the changes it causes on the airfoil's rotational acceleration and pitch dynamically:

$$L(p - l)cos\,\alpha + F_x l sin\,\alpha - F_y cos\,\alpha = I_G\frac{d^2\alpha}{dt^2}$$

where $L(p - l)cos\,\alpha$ is the moment produced by the lift force about the pivot, $F_x sin\,\alpha$ is the horizontal force which aids in rotation, $F_y cos\,\alpha$ is the vertical force opposing rotation and $I_G\frac{d^2\alpha}{dt^2}$ is the sum of moments acting about the pivot where I_G is the moment of inertia and $\frac{d^2\alpha}{dt^2}$ is angular acceleration.

Now, substitute the values of F_x and F_y. Upon simplifying we achieve:

$$(I_G + ml^2)\frac{d^2\alpha}{dt^2} + (g + \frac{d^2y}{dt^2})mlcos\,\alpha - (Lcos\,\alpha)p - Ml = 0$$

where $(I_G + ml^2)\frac{d^2\alpha}{dt^2}$ is the total inertial torque moment, $(g + \frac{d^2y}{dt^2})mlcos\,\alpha$ is the moment due to gravitational and vertical accelerative forces, $(Lcos\,\alpha)p$ is the lift induced moment and Ml is the constant moment term due to the airfoils body. This equation models the overall effect of the moments caused by F_x, F_y and lift on the rotational acceleration of the rigid body framework.

State Space Representation

State Space allows people to model multiple inputs simultaneously in one cohesive system. Therefore, allowing them to determine how they influence each other and how varying and changing the inputs affects the system. In this case, state space can help us to calculate the required torque and angular acceleration. Thus, engine gimbal angle to regain vertical orientation (Patel et al., 2026).

The fundamental equation for this representation is as follows where s is the state vector and u is the input:

$$\dot{s} = As + Bu$$

Modelling this equation by using the 4 variables α, $\dot{\alpha}$, y, $\dot{y}$:

$$\begin{bmatrix}\dot{\alpha}\\ \ddot{\alpha}\\ \dot{y}\\ \ddot{y}\end{bmatrix} = \begin{bmatrix}0 & 1 & 0 & 0\\ A & 0 & 0 & 0\\ 0 & 0 & 0 & 1\\ 0 & 0 & 0 & 0\end{bmatrix}\begin{bmatrix}\alpha\\ \dot{\alpha}\\ y\\ \dot{y}\end{bmatrix} + \begin{bmatrix}0\\ 0\\ 0\\ 1\end{bmatrix}\ddot{y}$$

Where the first column is the derivatives of the state variables representing their rate of change. The second column is the system matrix portraying how the system evolves over time and how the variables affect each other. Column three is the state variables. Column 4 is the input matrix depicting how the input influences the variables, and column five is the input to variables in the system.

To acquire values for the second row of the state-space representation, we rearrange the equation modeling the entire moment of the system:

$$\ddot{\alpha} = \frac{[Ml + Lp\,cos\,\alpha - mgl\,cos\,\alpha - mlcos\,\alpha\frac{d^2y}{dt^2}]}{I_G + ml^2}$$

State-space Representation Approaches

There are two approaches that can be used for the state-space representation. The first approach is a small angle approximation, where any non-linear terms are removed. Thereby, forming a linear equation which

can be written in the standard form of $\dot{s} = As + Bu$. Essentially, this approach linearises the equation near equilibrium, so $sin\ \alpha$ and $cos\ \alpha$ can be written as:

$$sin\ \alpha \approx \alpha$$
$$cos\ \alpha \approx 1$$

Therefore, $\ddot{\alpha}$ can be expressed by:

$$\ddot{\alpha} = \frac{[Ml + Lp - mgl - ml\frac{d^2y}{dt^2}]}{I_G + ml}$$

Where $\ddot{\alpha}$ is the angular acceleration, Ml is the torque from the airfoil's body, Lp is torque produced from lift, mgl is gravitational torque, $ml\frac{d^2y}{dt^2}$ is the coupling term, and $I_G + ml$ is the total rotational inertia.

However, the limitation to this approach is its inaccuracy at higher angles of attack as higher-order terms are neglected. This is because they only work effectively near equilibrium. Therefore, if the angle is too large, the restorative forces and coupling terms calculated will be incorrect.

In the second approach, the state variable is redefined. Thus, non-linear terms can be treated as states. As a result this would improve how the inputs interact within the dynamic system. Instead of having $cos\ \alpha$ as a non-linear function, it is treated as a state variable. This allows for enhanced coupling with inputs from the LQR feedback loop as the input will have a greater effect on the states.

$$\begin{bmatrix} \alpha \\ \dot{a} \\ y \\ \dot{y} \end{bmatrix} \rightarrow \begin{bmatrix} \cos\alpha \\ \dot{\alpha} \\ y \\ \dot{y} \end{bmatrix}$$

However, approach 2 does not completely linearize the variables as if $cos\ \alpha$ is treated as a state variable, its rate of change or derivative would be $-\ sin\ \alpha\ \times\ \dot{\alpha}$ which is non-linear, therefore this approach would not allow us to write the standard state space linear equation in the form $\dot{s} = As + Bu$, or would require extensive derivation to make it compatible with standard linear state-space form.

To meet the conditions for the system to be controllable, the study uses approach one. By the use of small angle approximations, the system meets the requirements of linearity so the linear state-space equation can be used which is compatible with standard LQR control techniques (Friedland, 2005). Applying approach one into the derived equations of motion outputs the numerical system matrices A and B:

$$A\ matrix = \begin{bmatrix} 0 & 1 & 0 & 0 \\ 99.5062 & 0 & 0 & 0 \\ 0 & 0 & 0 & 1 \\ 0 & 0 & 0 & 0 \end{bmatrix} \quad \text{B matrix} = \begin{bmatrix} 0 \\ -2.5 \\ 0 \\ 1 \end{bmatrix}$$

State-space Representation Controllability

Controllability of the system is primarily dependent on the rank of the controllability matrix. The controllability matrix enables us to determine whether all the state variables can be controlled through an input, and is defined as:

$$C = [B\ AB\ A^2B\ A^3B \ldots\ A^{n-1}B]$$

Where A is the system matrix, B is the input matrix and n is the number of states in the system. B illustrates the effect the direct input has on the system, AB demonstrates how the input effects the system after one step of system dynamics and so on until AB^{n-1}.

The essential condition for system controllability is:

$$Rank\ (C) = n$$

Since our system has 4 different state variables, the essential condition for the controllability of the system is:

$$Rank\ (C) = 4 \text{ (full rank)}$$

Controller Design

A Linear Quadratic Regulator (LQR) controller was chosen over traditional PID controllers due to its multivariable nature. Where PID controllers produce an output solely based upon the data available in front of it using single loop control where each feedback loop is designated for a different variable, LQR controllers commence a series of calculations to produce a corrective input using a closed multivariable feedback loop where outputs are evaluated against the desired value. Thus, optimising its output to eventually achieve the required setpoint. The LQR framework was coded in python and implemented the controllability matrix. Thereby, allowing us to determine whether the system had a full rank which was equal to 4. Therefore, the correct gain value can be calculated returning the cart to its vertical orientation.

Table 1: Physical numerical system parameters for the LQR controller

Parameter	Symbol	Value	Unit
Airfoil mass	m	0.5	kg
Cart mass	M	1	kg

Gravitational acceleration	g	9.81	$\frac{m}{s^2}$
Pivot to CM distance	l	0.3	m
Viscous damping coefficient	b	0.05	$\frac{N \cdot s}{m}$
Chord length	c	0.3	m
Aerodynamic moment arm	p	0.225	m
Moment of inertia about CM	I_G	0.015	$kg \cdot m^2$
Air density	ρ	1.225	$\frac{kg}{m^3}$
Freestream velocity	V_∞	15	$\frac{m}{s}$
Lift coefficient	C_l	0.8	-
Q matrix	Q	$Q = \begin{bmatrix} 10 & 0 & 0 \\ 0 & 1 & 0 \\ 0 & 0 & 1 \\ 0 & 0 & 0 \end{bmatrix}$	-
R matrix	R	$R = 0.5$	-

The system is initially linearised allowing us to model the system in the state-space form $\dot{s} = As + Bu$, where the state variables are $[\alpha, \dot{\alpha}, y, \dot{y}]$ and the input is the acceleration of the cart in the flow field where $u = \ddot{y}$. In addition, implemented into the code is a section for controllability. The system will only function correctly and calculate the correct gain values if the controllability matrix Rank is full (Rank = 4). Therefore a designated line in the code output informs us on the system's controllability matrix rank, ensuring coupling between variables and that the input affects their magnitude (Patel et al., 2026). Then, the LQR network is introduced by using the weighting matrices Q and R. This is where Q is the diagonal weighting matrix which castigates angular deviations, such as velocity and pitch angle. The following code excerpt demonstrates the implementation of LQR controller design using the control library:

```
#LQR Controller Design:
Q = np.diag([10, 1, 10, 1])
R = np.array([[0.5]])

K, S, E = ctl.lqr(A_4, B_4, Q, R)
```

Excerpt 1: LQR implementation using Python control library

Utilising larger Q matrix values will result in more aggressive control attempts where larger forces may act (Patel et al., 2026). While this could result in reduced settling time, it may cause overshoot and reduce system efficiency and fuel consumption. This is where matrix R comes in which is the managing control effort matrix. Increasing R matrix values produces less jolty and aggressive movements. Thereby, enabling a slower but smoother control. Next, the feedback loop gain matrix K is calculated by using computational tools which solve the riccati equation. The output of this state feedback loop is a gain value K:

$$Optimal\ LQR\ Gain\ K = [-110.13,\ -11.12,\ -4.47,\ -4.22]$$

After the gain value K is calculated, the controller uses a feedback loop to continuously reevaluate the state variables creating a closed-loop system to correct the variables to the required setpoint. A visualisation is used to model the dynamic system returning to equilibrium (Patel et al., 2026). The following code excerpt demonstrates this closed-loop system:

```
#Closed-Loop System:

sys4 = ctl.ss(A_4, B_4, C_4, D_4)
sys4CL = ctl.feedback(sys4, K)
```

Excerpt 2: Closed feedback loop system

FINDINGS AND DISCUSSION

To evaluate the performance and robustness of the LQR controller, we can analyse its speed and efficiency in returning the cart to the equilibrium setpoint (vertical orientation) by using time simulations. Through replicating possible initial non-zero conditions for the pitch, pitch rate, cart position and cart velocity, the potency and success of the controller can be assessed. A robust and efficient controller should provide a quick and non-oscillatory response motion (Patel et al., 2026). Oscillatory motion can occur due to a gap in the controllability of the state variables, or the omittance of a damping term. If the state variables are completely disconnected from the input variable, then no matter the force applied on the system, no change will occur to the state variables. This issue may be addressed by ensuring sufficient coupling of the system dynamics with the input variable through iterative definition of control inputs, or

insertion of missing physical parameters. In addition, oscillation can be minimised through the introduction of a sufficient damping term. A damping term is a force or in code a mathematical value that opposes the motion of a cart in a flow field and drains the system of energy, transferring it to other stores. Without this value the state variables would oscillate forever.

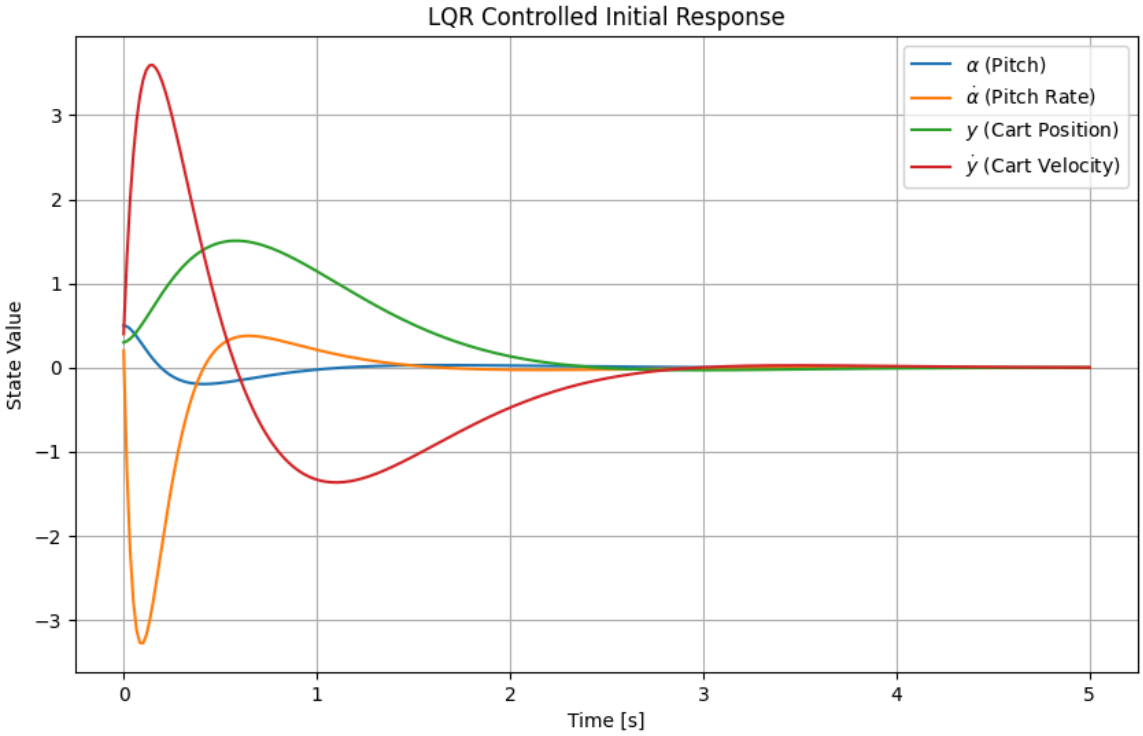

Figure 3: demonstrates how the dynamic variables pitch, pitch rate, cart position and cart velocity change overtime using gain values calculated from the LQR controller until equilibrium is reached $(State\ Value = 0)$ **at a time domain of 10 seconds.**

The closed feedback loop allows the LQR to constantly update its gain values and damping terms which are produced from changes in pitch rate and cart velocity, as modelled in Figure 3. A large and rapid acceleration upwards of the trailing edge can be witnessed. Thus, enabling the required restorative torque moments to be produced. Then, the LQR reverses the input direction and calculates a new gain value to return the system to equilibrium. This loop repeats until the cart reaches an angle of attack to the vertical of 0 degrees (Patel et al., 2026). By changing initial system parameters, such as the distance between the pitch axis and centre of mass, or the mass of the cart, we are able to evaluate the importance of maintaining the correct system parameters on LQR efficiency and usefulness. As the centre of mass is closer to the trailing edge of the aerial vehicle a greater restorative torque moment can be produced. Thereby, allowing the calculated gain value to be optimised for thrust vector control to commence with the vertical attitude adjustments.

The time taken for the cart to reach the desired vertical position $y = 0$ may be reduced by increasing the state penalties applied to the variables. The state variables with the greatest influence on the cart's orientation are pitch angle and cart position. By increasing the weighting of these state variables they can react more aggressively, reducing settling time. In addition, by reducing control penalty stronger inputs can be made allowing the controller to use larger restorative forces. However, this can cause overshoot, reducing the accuracy and robustness of the control system and may not align with realistic actuator capabilities.

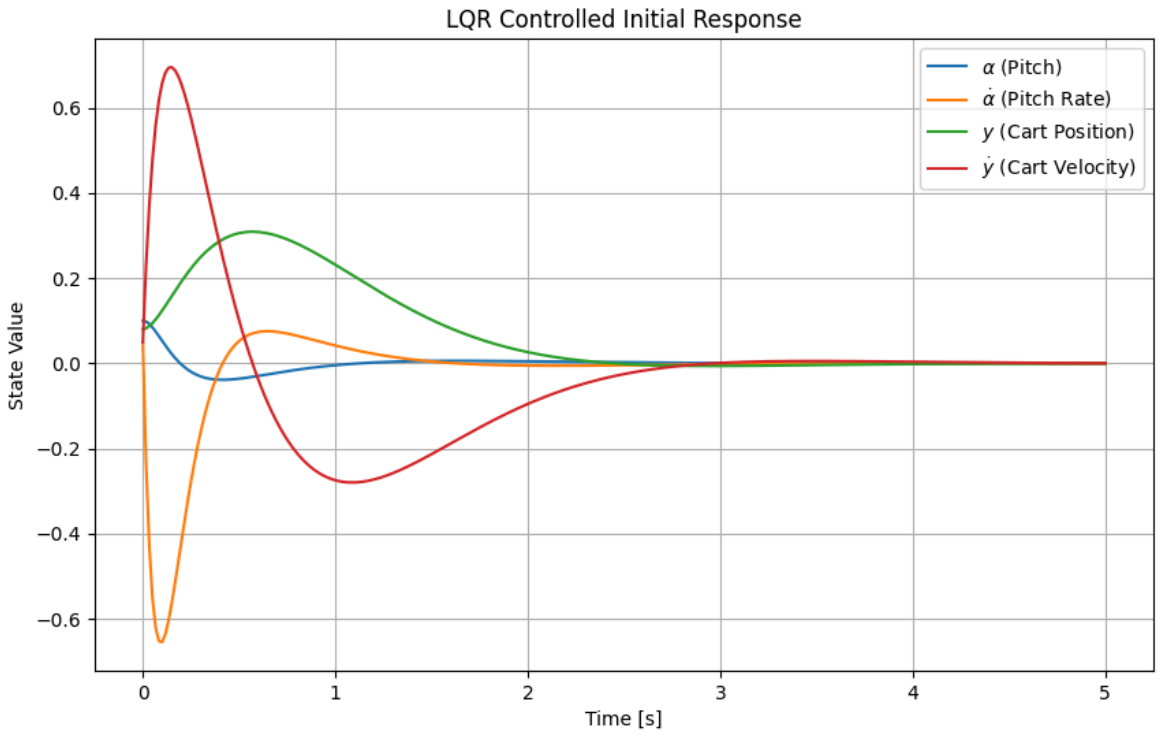

Figure 4 highlights the same LQR controller design with altered initial conditions and physical system parameters compared to the graph shown in the previous figure. Where the previous graph demonstrates a system with large initial disturbances requiring large forceful intervention from the LQR, this graph exhibits a system with a smaller initial velocity and perturbations as suggested by the difference in y-axis values between the graphs.

To further evaluate the performance of the LQR controller, a graph can be modelled by illustrating a cart moving vertically upwards in a flow field, with initial disturbance conditions induced on its body. Therefore, enabling people to envision the effects the CM has on LQR accuracy and performance. This is where as the distance from the CM of the cart to the pivot point decreases, LQR performance is drastically reduced. This can be explained by using the moment equation where $moment = force \times distance$, as the distance is decreased, a much greater force is required to create

an identical restorative torque moment. Therefore, leading to calculated gain values being more large and aggressive which can lead to controller overshoot and unnecessary oscillatory motion.

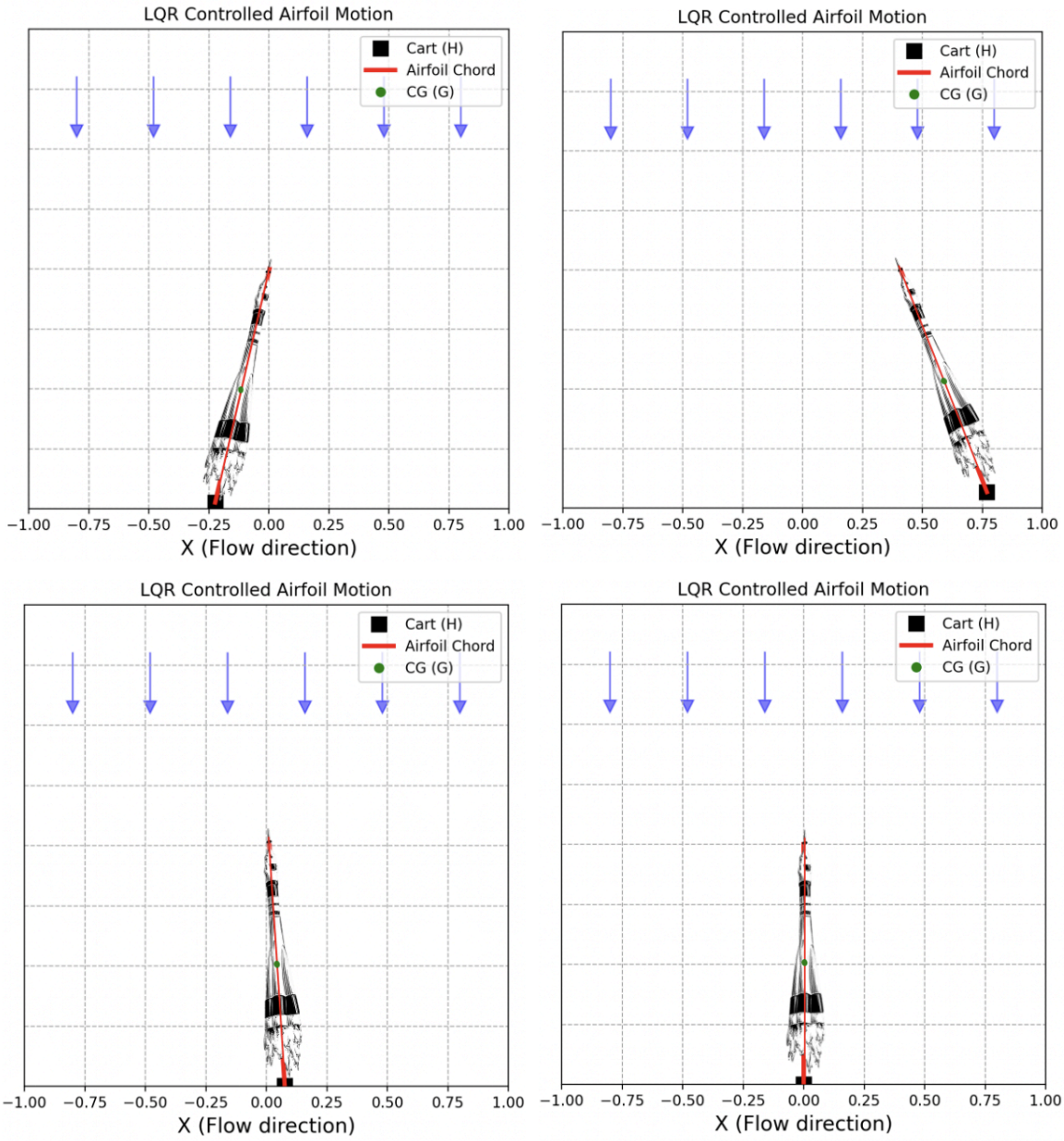

Figure 5 demonstrates a visualisation of a cart in a flow field experiencing initial disturbance conditions, and how overtime using gain values and damping terms calculated from the LQR controller the cart is able to achieve the desired vertical orientation at $y = 0$.

CONCLUSION

Through using graphs and findings that were gathered from the LQR controller with differing conditions and system parameters, it can be concluded that Linear Quadratic Regulators are efficient and dependable tools. They can be implemented into modern rocketry control systems and design to help govern the attitude of aerial vehicles. This is especially during the launch phase of aerospace rockets where launch success is central to the triumph of the mission. However, it must also be recognised that if the initial conditions and physical parameters acting on the rocket are too large or outside the LQR's best suited range, its accuracy may decrease leading to unwanted and unregulated swaying motion. This would place extra stresses on the fuselage, and ultimately the inability to efficiently return the aerial vehicle to the required vertical orientation.

Through the dual evaluation of PID vs LQR controller design, the research has highlighted the pragmatic nature of the LQR's multivariable complexion. This is where the LQR is able to optimise system dynamics and TVC actions to minimise effort, and reduce unwanted motion through informed calculations. This is unlike the PID controller where system guidance is governed solely through available data. Therefore, for modern aerospace systems where precision is a key principle and margins of error are fundamentally zero, LQR design provides the most compatible approach and optimal framework. This is because the linearisation of system dynamics allows for the capture of coupled variables such as in the pitch and yaw axes, where the variables can be controlled simultaneously. Thereby providing an efficient and energy conscious control model.

However, while the LQR system may excel at smaller angles of attack, as the angle increases perhaps due to compressor stall the system dynamics may include higher order values and become non-linear. Therefore, an LQR framework may be unable to capture and control these variables. To resolve this issue gain scheduling may be implemented, where an autonomous LQR model is designed for a certain range of the angle of attack, creating a treasury of LQRs, each for a different range of angles. While this does provide a robust solution, it may be expensive and as there are more control entities uncertainties may rise.

The implications of the LQR controller extend past rockets exclusively. They can expand into the larger aerospace industry and government use in commercial aircraft, such as the mitigation of compressor stall in turbofan planes, like the Boeing 777 or the Airbus A380. While the LQR controller does provide an efficient and adaptive process to regain the preferred orientation, its implementation into the industry requires tactical dismantle and reconfiguration for the specified use, strategic technologies and bureaucratic supervision. The LQR should not be utilised as an independent controller. It should be combined with other guidance systems, such as Model Predictive Control (MPC) controllers, which predict the nature of the commencing movement. Thereby, providing a more infallible and robust output. In addition, if these controllers were to be considered for commercial use, regulatory measures must be taken to ensure the safety of passengers and prevent cyberattacks or hacking of these systems.

Finally, the LQR contributes to a sustainable future through its optimised outputs where the motion of the fuselage is minimised. Thereby, reducing fuel consumption and energy costs, producing a more fuel-efficient vehicle. Through government adoption of the LQR control system further research may be incentivised by approved research centres on the measures required for these methodical networks to work innately.

References

[1] Aerotecnica. (2023). *ADCS Design for a Sounding Rocket with Thrust Vectoring.* Aerotecnica Missili & Spazio. https://link.springer.com/article/10.1007/s42496-023-00161-w?utm_source=chatgpt.com#Sec1

[2] Apogee Components. (n.d.). *Insights - Parts of a Rocket.* Apogee Components Educates. https://www.apogeerockets.com/downloads/PDFs/Insights-Parts.pdf

[3] CalAcademy. (n.d.). *Anatomy of a Rocket.* California Academy of Sciences. https://www.calacademy.org/sites/default/files/assets/docs/calacademy-sah-rockets-anatomy_of_a_rocket-210415.pdf

[4] Ekanayake, I. (2026). *Structural Design & Load Management of Rocketry.* https://medium.com/@sedsjapura/structural-design-load-management-of-rocketry-af166b8e24ee

[5] Embry-Riddle. (n.d.). *Introduction to Aerospace Flight Vehicles - Rockets and Launch Vehicles.* https://eaglepubs.erau.edu/introductiontoaerospaceflightvehicles/chapter/rocket-performance/

[6] Friedland, B. (2005). *Control System Design: An Introduction to State-Space Methods.* https://www.academia.edu/16854890/Control_System_Design_An_Introduction_to_State_Space_Methods_Bernard_Friedland_Dover_Publications_?sm=b&rhid=40629483999

[7] Glenn. (2023). *Beginners guide to Aeronautics - Rocket Control.* Glenn Research Centre. https://www1.grc.nasa.gov/beginners-guide-to-aeronautics/rocket-control/

[8] Glenn. (2023). *Beginners Guide to Aeronautics - Rocket Parts.* Glenn Research Center. https://www1.grc.nasa.gov/beginners-guide-to-aeronautics/rocket-parts/#guidance-system

[9] Jang, J. W. et al. (2011). *Design of Launch Vehicle Flight Control Systems Using Ascent Vehicle Stability Analysis Tool.* https://ntrs.nasa.gov/api/citations/20110015701/downloads/20110015701.pdf

[10] National. (2021). *Practical Rocketry.* National Aeronautics and Space Administration (NASA). https://www.grc.nasa.gov/www/k-12/rocket/TRCRocket/practical_rocketry.html

[11] National. (2021). *Brief History of Rockets.* National Aeronautics and Space Administration (NASA). https://www.grc.nasa.gov/www/k-12/rocket/TRCRocket/history_of_rockets.html

[12] National. (2021). *Rocket Principles.* National Aeronautics and Space Administration (NASA). https://www.grc.nasa.gov/www/k-12/rocket/TRCRocket/rocket_principles.html

[13] National. (2024). *95 Years Ago: Goddard's first Liquid-Fueled Rocket.* National Aeronautics and Space Administration (NASA). https://www.nasa.gov/history/95-years-ago-goddards-first-liquid-fueled-rocket/#:~:text=Goddard.-,Robert%20H.,a%20farm%20in%20Auburn%2C%20Massachusetts.

[14] Neufeld, M. (2016). *Robert Goddard and the First Liquid-Propellant Rocket.* https://airandspace.si.edu/stories/editorial/robert-goddard-and-first-liquid-propellant-rocket

[15] Patel, Y, Simon, S, & Dawson, S. T. M. (2026). *The Aerodynamic Inverted Pendulum: Modeling and Stabilization of a Trailing-Edge–Hinged Airfoil*. https://www.researchgate.net/publication/400226976_The_Aerodynamic_Inverted_Pendulum_Modeling_and_Stabilization_of_a_Trailing-Edge-Hinged_Airfoil

[16] Patel, Y & Ansell, P. J. (2023). *Airfoil Performance Sensitivity to Laminar Separation Bubble Topology.* https://www.researchgate.net/publication/371441965_Airfoil_Performance_Sensitivity_to_Laminar_Separation_Bubble_Topology

[17] Sutton, G. P. & Biblarz, O. (2017). *Rocket Propulsion Elements Ninth edition.* https://ftp.idu.ac.id/wp-content/uploads/ebook/tdg/DESIGN%20SISTEM%20DAYA%20GERAK/Rocket%20Propulsion%20Elements.pdf

[18] Sheth, S. et al. (2024). *A Computational Analysis of Jet Vanes Thrust Vector Control for Solid Rocket Propulsion. https://arc.aiaa.org/doi/epdf/10.2514/6.2024-85701*

[19] Sopegno, L. et al. (2023). *Thrust Vector Controller Comparison for a Finless Rocket.* https://www.mdpi.com/2075-1702/11/3/394

[20] GU. (2021). *Rocket Aerodynamics - Sutton Program Article 5.* GU Rocketry. https://www.rs-online.com/designspark/rocket-aerodynamics-sutton-program-article-5

[21] SimScale. (n.d.). *What is Lift, Drag and Pitch in Aerodynamics?* SimScale. https://www.simscale.com/docs/simwiki/lift-drag-pitch/

[22] Nakka, R. (2023). *Introduction to Rocket Design.* https://www.nakka-rocketry.net/RD_nosecone.html

[23] Åström, K, J. (2002). *Control System Design.* https://www.cds.caltech.edu/~murray/courses/cds101/fa02/caltech/astrom.html

[24] ScienceDirect. (n.d.). *Linear Quadratic Regulator.* ScienceDirect. https://www.sciencedirect.com/topics/physics-and-astronomy/linear-quadratic-regulator